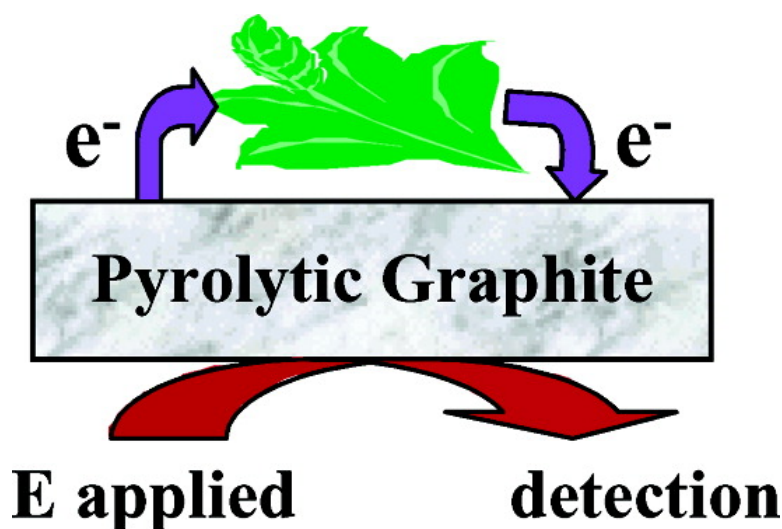


## Electron Transfer Reactions of Redox Cofactors in Spinach Photosystem I Reaction Center Protein in Lipid Films on Electrodes

Bernard Munge, Somes K. Das, Robielyn Ilagan, Zeus Pendon, Jing Yang, Harry A. Frank, and James F. Rusling

*J. Am. Chem. Soc.*, **2003**, 125 (41), 12457-12463 • DOI: 10.1021/ja036671p • Publication Date (Web): 20 September 2003

Downloaded from <http://pubs.acs.org> on March 29, 2009



### More About This Article

Additional resources and features associated with this article are available within the HTML version:

- Supporting Information
- Links to the 5 articles that cite this article, as of the time of this article download
- Access to high resolution figures
- Links to articles and content related to this article
- Copyright permission to reproduce figures and/or text from this article

[View the Full Text HTML](#)

## Electron Transfer Reactions of Redox Cofactors in Spinach Photosystem I Reaction Center Protein in Lipid Films on Electrodes

Bernard Munge,<sup>†</sup> Somes K. Das,<sup>†</sup> Robielyn Ilagan,<sup>†</sup> Zeus Pendon,<sup>†</sup> Jing Yang,<sup>†</sup> Harry A. Frank,<sup>\*,†</sup> and James F. Rusling<sup>\*,†,‡</sup>

Contribution from Department of Chemistry, University of Connecticut, Storrs, Connecticut 06269-3060, and Department of Pharmacology, University of Connecticut Health Center, Farmington, Connecticut 06032

Received June 13, 2003; E-mail: James.Rusling@uconn.edu.

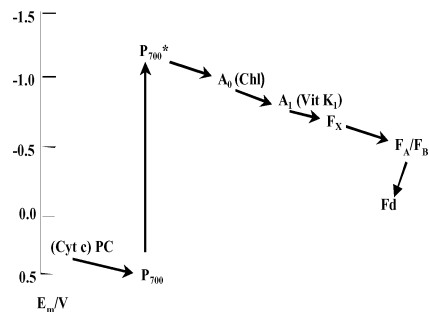
**Abstract:** Thin film voltammetry was used to obtain direct, reversible, electron transfer between electrodes and spinach Photosystem I reaction center (PS I) in lipid films for the first time. This reaction center (RC) protein retains its native conformation in the films, and AFM showed that film structure rearranges during the first several minutes of rehydration of the film. Two well-defined chemically reversible reduction–oxidation peaks were observed for native PS I in the dimyristoylphosphatidylcholine films, and were assigned to phylloquinone,  $A_1$  ( $E_m = -0.54$  V) and iron–sulfur clusters,  $F_A/F_B$  ( $E_m = -0.19$  V) by comparisons with PS I samples selectively depleted of these cofactors. Observed  $E_m$  values may be influenced by protein–lipid interactions and electrode double-layer effects. Voltammetry was consistent with simple kinetically limited electron transfers, and analysis of reduction–oxidation peak separations gave electrochemical rate constants of  $7.2$  s<sup>-1</sup> for  $A_1$  and  $65$  s<sup>-1</sup> for  $F_A/F_B$ . A catalytic process was observed in which electrons were injected from PS I in films to ferredoxin in solution, mimicking in vivo electron shuttle from the terminal  $F_A/F_B$  cofactors to soluble ferredoxin during photosynthesis.

### Introduction

Initial steps in photosynthesis to convert light energy into chemical energy in plants, green algae, and cyanobacteria occurs via Photosystem I (PS I), a large transmembrane protein-cofactor complex.<sup>1,2</sup> PS I converts light into reducing power to drive the endergonic reduction of NADP<sup>+</sup> to NADPH.<sup>3</sup> The resulting strong reducing agent, NADPH in conjunction with the bio-synthesized photophosphorylation energy from ATP is used to fix carbon in the Calvin cycle.<sup>4</sup> In this way, light energy converts carbon dioxide into sugar, starch, and other high-energy carbohydrates on which the entire biosphere depends. Highly resolved (2.5 Å) X-ray crystal structures<sup>2,5</sup> of PS I from cyanobacteria revealed a trimer with each subunit containing 12 different proteins binding 96 chlorophylls and more than 30 other cofactors.

Upon photoexcitation of the primary electron donor (P700), a chlorophyll dimer in PS I, a series of one-electron-transfer steps occur (Scheme 1). Electron acceptors include a chlorophyll monomer ( $A_0$ ), phylloquinone ( $A_1$ , Vitamin K<sub>1</sub>), and three iron–

**Scheme 1.** Electron Transfer Pathways for PS I<sup>a</sup>



<sup>a</sup> Approximate midpoint potentials (vs SHE) for the various redox centers in PS I as discussed in the text are shown on the scale at the left. Adapted from ref 15.

sulfur [4Fe–4S] clusters ( $F_X$ ,  $F_A$ , and  $F_B$ ), and midpoint potentials have been estimated in some cases by mediated redox titrations. Electrons from  $F_A/F_B$  are donated to soluble ferredoxin (Fd), which shuttles them to ferredoxin:NADP<sup>+</sup> reductase to catalyze the reduction of NADP<sup>+</sup>.<sup>3</sup> The oxidized chlorophyll dimer ( $P700^+$ ) is rereduced by a soluble protein, plastocyanin (PC) or cytochrome *c*.<sup>6,7</sup>

Electrochemical interrogation of plant PS I and PS II is a major challenge that may lead to detailed fundamental characterization of the numerous redox cofactors. Immobilization of photosynthetic reaction center proteins on metal surfaces, on

<sup>†</sup> Department of Chemistry, University of Connecticut.

<sup>‡</sup> Department of Pharmacology, University of Connecticut Health Center.

(1) Zak, E.; Norling, B.; Maitra, R.; Huang, F.; Anderson, B.; Pakrasi, H. B. *Proc. Natl. Acad. Sci.* **2001**, *23*, 13 443–13 448.

(2) Jordan, P.; Fromme, P.; Klukas, O.; Witt, H. T.; Saenger, W.; Krauss, N. *Nature* **411**, **2001**, 909–917.

(3) Lakshmi, K. K.; Jung, Y.-S.; Golbeck, J. H.; Brudvig, G. W. *Biochemistry* **1999**, *38*, 13 210–13 215.

(4) Calvin, M. *Science* **1962**, *135*, 879–889.

(5) Fromme, P.; Jordan, P.; Krauss, N. *Biochim. Biophys. Acta.* **2001**, *1507*, 5–31.

(6) Stryer, L. *Biochemistry*; Freeman, New York, 1981.

(7) Golbeck, J. H. *Annu. Rev. Plant Physiol. Plant. Mol. Biol.* **43**, **1992**, 293.

electrodes, or between capacitor plates has been reported previously, with applications including measurement of photocurrents or photovoltages,<sup>8</sup> investigation of electric-field effects on light-induced charge separation,<sup>9</sup> and inducing surface-enhanced Raman spectra.<sup>10</sup> Differing in aim from these previous reports, our goal in the present paper was to directly address the redox cofactors of PS I by voltammetry. Previously, only small, barely detectable, diffusion-controlled cyclic voltammetry peaks for detergent-solubilized PS I were observed at promoter-modified Au electrodes, and these were assigned to the P700 cofactor.<sup>11</sup>

Thin film voltammetry has become a method of choice for studying the redox properties of proteins.<sup>12</sup> In this method, proteins are entrapped in monolayers or multilayers on electrode surfaces, often with coadsorbate, so that diffusion of these large species to electrodes is not a limiting factor. The high local concentration of protein sequestered on the electrode surface can give much larger and better defined voltammetric peaks than for the same proteins in solution. In many cases, direct electron exchange between proteins and electrodes can be achieved in these films without electron-transfer mediators. For example, we have reported direct voltammetry of soluble proteins myoglobin,<sup>13</sup> and cytochrome P450<sub>cam</sub><sup>14</sup> in layered self-assembled lipid films, and in layered protein-polyion films.<sup>16,17</sup> Recently, we reported irreversible electrochemical reactions of redox cofactors within the photosynthetic reaction center of the purple bacterium *Rhodobacter sphaeroides* in lipid films.<sup>18</sup> Using thin layer voltammetry along with selective removal of cofactors, we were able to identify peaks for the primary electron donor (P860) and quinones, and documented the influence of light and the catalytic reaction of P860<sup>+</sup> with cyt c.

We set out in the present work to achieve direct electrical communication between electrodes and photosynthetic reaction center proteins from higher plants. In this paper, we report the first example of direct, reversible voltammetric reduction—

oxidation peaks for two cofactors within the spinach membrane protein complex PS I in lipid films. By selectively depleting the cofactors in special preparations of PS I, we assigned these reversible peaks to the cofactors phyloquinone A<sub>1</sub> and the iron sulfur clusters F<sub>A</sub>/F<sub>B</sub>. Also, electron donation from the electron acceptor cofactors F<sub>A</sub>/F<sub>B</sub> to the iron–sulfur protein ferredoxin in solution was observed.

## Experimental Section

**Chemicals and Materials. Native PS I Reaction Center (RC).** PS I from spinach was isolated according to literature procedures,<sup>19,20</sup> and used in pH 8 Tris buffer (0.5 mg/mL). For film construction, the PS I particles obtained from the destacked thylakoid membrane were suspended in 150 mM NaCl to give 0.6 mg mL<sup>-1</sup> chlorophyll followed by mixing with an equal volume of 2.0% *n*-dodecyl- $\beta$ -D-maltoside (DM, Calbiochem) while stirring on ice for 5 min. Then, 0.5–1.0 mL aliquots were loaded onto 10–40% sucrose gradients containing 5 mM Tricine, 150 mM NaCl, 0.5% DM at pH 7.8 and centrifuged at 285 000  $\times$  g for 30 h at 4 °C using a Beckman SW40 rotor. The lowest three bands containing PS I reaction centers were collected and dialyzed overnight in 50 mM Tris buffer at pH 8.3.<sup>20</sup> The protein was concentrated using a YM-100 concentrator, then washed with 50 mM Tris buffer at pH 8.3 to remove the detergent and the final chlorophyll (Chl) concentration adjusted to 0.5 mg mL<sup>-1</sup>.

Dimyristoylphosphatidylcholine (DMPC, >99%) and spinach ferredoxin (Fd, MW 15 Kda, ~25% ferredoxin by wt.) were from Sigma. Water was treated with a Hydro Nanopure purification system to specific resistivity >16 m $\Omega$ -cm. All other chemicals were reagent grade.

**PS I Depleted of F<sub>A</sub> and F<sub>B</sub> Cofactors.** Using a literature method,<sup>21,22</sup> the concentrated PS I particles containing P700, A<sub>0</sub>, A<sub>1</sub>, F<sub>A</sub>, F<sub>B</sub>, and F<sub>X</sub> cofactors were mixed with equal volume of a solution containing 0.2 M glycine, 10 M urea at pH 10.0, to give a final Chl concentration of 0.25 mg/mL.<sup>21,22</sup> The reaction mixture was allowed to react at room temperature for 10 min followed by 15 h dialysis in 50 mM Tris at pH 8.3. The dialyzed sample was concentrated to half the original volume, then 1–2 mL of this concentrated solution loaded onto 0.1 to 1.0 M sucrose gradient tubes containing 50 mM Tris and 0.1% Triton X-100 at pH 8.3 followed by centrifuging for 25 h at 115 000  $\times$  g using 55.2 Ti rotor. Finally, the resulting lower green band containing the reaction center with P700, A<sub>0</sub>, A<sub>1</sub>, F<sub>X</sub>, but depleted of F<sub>A</sub> and F<sub>B</sub> was collected using a syringe and dialyzed overnight in 50 mM Tris at pH 8.3 at 4 °C, then concentrated and stored at –80 °C in 20% glycerol.

**PS I Depleted of F<sub>A</sub>, F<sub>B</sub>, and F<sub>X</sub>.** Briefly, the native PS I reaction center, at a concentration of 0.25 mg/mL was incubated for 3 h with 3 M urea and 5 mM K<sub>3</sub>Fe(CN)<sub>6</sub> in 50 mM Tris at pH 8.3.<sup>23</sup> Then, excess urea and K<sub>3</sub>Fe(CN)<sub>6</sub> were removed by overnight dialysis in 50 mM Tris at pH 8.3, whereas excess iron was removed by 15 h dialysis in 50 mM Tris, pH 8.3, containing 5 mM Tiron (disodium 4,5-dihydroxy-1,3-benzene-

- (8) For examples see (a) Lee, I.; Lee, J. W.; Warmack, R. J.; Allison, D. P.; Greenbaum, E. *Proc. Natl. Acad. Sci. U.S.A.* **1995**, *92*, 1965–1969. (b) Lee, J. W.; Lee, I.; Greenbaum, E. *Biosens. Bioelect.* **1996**, *11*, 375–387 and references therein. (c) Lee, I.; Lee, J. W.; Greenbaum, E. *Phys. Rev. Lett.* **1997**, *79*, 3294–3297. (d) Yasuda, Y.; Kawakami, Y.; Toyotama, H. *Thin Solid Films* **1997**, *292*, 198–191. (e) Lee, I.; Lee, J. W.; Stubna, A.; Greenbaum, E. *J. Phys. Chem. B*, **2000**, *104*, 2439–2443.
- (9) Moser, C. C.; Sension, R. J.; Szarka, A. Z.; Repinec, S. T.; Hochstrasser, R. M.; Dutton, P. L. *Chem. Phys.* **1995**, *197*, 343–354.
- (10) (a) Picorel, R.; Holt, R. E.; Heald, R.; Cotton, T. M.; Seibert, M. *J. Am. Chem. Soc.* **1991**, *113*, 2839–2843. (b) Picorel, R.; Chumanov, G.; Montoya, G.; Cotton, T. M.; Toon, S.; Seibert, M. *J. Phys. Chem.* **1994**, *98*, 6017–6022.
- (11) Kievet, O.; Brudvig, G. W. *J. Electroanal. Chem.* **2001**, *497*, 139–149.
- (12) (a) Armstrong, F. A.; Heering, H. A.; Hirst, J. *Chem. Soc. Rev.* **1997**, *26*, 169–179. (b) Armstrong, F. A. In *Bioelectrochemistry of Biomacromolecules*; Lenz, G., Milazzo, G., Eds.; Birkhauser Verlag: Basel, Switzerland, 1997; pp. 205–255. (c) Armstrong F. A.; Wilson, G. S. *Electrochim. Acta*, **2000**, *45*, 2623–2645. (d) Rusling, J. F.; Zhang, Z. In *Handbook Of Surfaces And Interfaces Of Materials, Vol. 5. Biomolecules, Biointerfaces, and Applications*; Nalwa, R. W., Ed.; Academic Press: New York, 2001, pp 33–71. (e) Rusling, J. F.; Zhang, Z. *Biomolecular Films*; in Rusling, J. F., Ed.; Marcel Dekker: New York, 2003, pp 1–64. (f) Niki, K.; Gregory, B. W. In *Biomolecular Films*; Rusling, J. F., Ed. Marcel Dekker: New York, 2003, pp 65–98.
- (13) Nassar, A.-E.; Zhang, Z.; Hu, N.; Rusling, J. F. *Phys. Chem. B* **1997**, *101*, 2224–2231.
- (14) Zhang, Z.; A.-E. Nassar, Z. Lu, J. B. Schenkman, J. F. Rusling *J. Chem. Faraday Trans.* **1997**, *93*, 1769–1774.
- (15) Ames, J., Ed.; *Photosynthesis, New Comprehensive Biochemistry Series, Vol. 15*; Elsevier: Amsterdam, 1987.
- (16) Lvov, Y. M.; Lu, Z.; Schenkman, J. B.; Zu, X.; Rusling, J. F. *J. Am. Chem. Soc.* **1998**, *120*, 4073–4080.
- (17) Munge, B.; Estavillo, C.; Schenkman, J. B.; Rusling, J. F. *ChemBioChem* **2003**, *4*, 82–89.
- (18) Munge, B.; Pendon, Z.; Frank, H. A.; Rusling, J. F. *Bioelectrochemistry* **2001**, *54*, 145–150.

- (19) Mullet, J. E.; Burke, J. J.; Arntzen, C. R. *Plant Phys.* **1980**, *65*, 814–822.
- (20) Bassi, R.; Simpson, D. *Eur. J. Biochem.* **1987**, *163*, 221–230.
- (21) Golbeck, J. H.; Parrett, K. G.; Mehari, T.; Jones, K. L.; Brand, J. J. *FEBS Lett.* **1988**, *228*, 268–272.
- (22) Parrett, K. G.; Warren, P. G.; Mehari, T.; Golbeck, J. H. *Biochim. Biophys. Acta* **1989**, *973*, 324–332.
- (23) Warren, P. V.; Parrett, K. G.; Warden, J. T.; Golbeck, J. H. *Biochemistry* **1990**, *29*, 6545–6550.

disulfonate). Residual Tiron and tiron-iron complex was removed by 15 h dialysis in 50 mM Tris, pH 8.3 containing 0.04% Triton X-100. Finally, the sample preparation containing P700, A<sub>0</sub> and A<sub>1</sub> was washed with 50 mM Tris at pH 8.3 in 0.04% Triton X-100 using a YM-100 concentrator and stored in 20% glycerol at -80 °C.

**PS I Depleted of F<sub>A</sub>, F<sub>B</sub>, F<sub>X</sub>, and A<sub>1</sub>.** Removal of F<sub>A</sub>, F<sub>B</sub>, F<sub>X</sub>, and A<sub>1</sub> was done according to literature.<sup>24–26</sup> Briefly, the original PS I reaction centers obtained from the DM treated thylakoids were concentrated to 200 μg Chl/mL using YM 30 membrane and mixed with an equal volume of 2% SDS.<sup>24</sup> Then the mixture was incubated for 2 h at room temperature followed by washing using YM-100 ultra filtration membrane to give 0.5 mg Chl/mL concentration. Then, 1–2 mL aliquots of this solution were centrifuged in a 0.1–1.0 M sucrose density gradient containing 50 mM Tris at pH 8.3 for 18 h at 115 000 × g and the lower green band containing protein binding P700 and A<sub>0</sub> was collected.<sup>25,26</sup> Finally, excess sucrose was removed by dialysis in 50 mM Tris at pH 8.3 with 0.02% Triton X-100 to give a sample containing 1 mg Chl/mL, which was stored in 20% glycerol at -80 °C.

**Characterization of PS I Materials.** The purity of native PS I reaction center was confirmed by SDS-PAGE as previously described.<sup>27</sup> SDS-PAGE was also used to assay the integrity of the preparations following treatment to remove selected redox cofactors. PS I preparations from spinach contain polypeptides which migrate on SDS-PAGE with apparent molecular masses of ~66, 18, 16, 14, and 9 kDa.<sup>21,28</sup> The 66 kDa band constitutes the P700 apoprotein. The 9 kDa band represents the apoprotein of F<sub>A</sub>/F<sub>B</sub>. In our preparations an additional band at ~100 kDa was seen and represents the P700-chlorophyll *a*-protein not converted to its homologous 66 kDa apoproteins. Although the absence of 9 kDa polypeptide in the iron sulfur protein-depleted PS I preparations is difficult to detect because it is known to stain only lightly with Coomassie brilliant blue,<sup>29</sup> the 18 kDa polypeptide, which is present in the native PS I preparation, disappears from both the F<sub>A</sub>/F<sub>B</sub> depleted PS I and F<sub>A</sub>/F<sub>B</sub>/F<sub>X</sub> depleted PS I preparations. A similar observation was reported by Golbeck et al.<sup>21</sup>

**Apparatus and Procedures. Film Preparation.** Basal plane pyrolytic graphite (PG, Advanced Ceramics) disk electrodes of geometric area 0.16 cm<sup>2</sup> were initially abraded with 600 grit SiC paper, then roughened using medium crystal bay (PH4 3M 001K) emery cloth, washed thoroughly with pure water followed by sonication in water for 30 s. The final area was 0.21 cm<sup>2</sup>.<sup>30</sup> DMPC-PS I films were prepared from vesicle dispersions of 2 mM dimyristoylphosphatidylcholine (DMPC) in pH 8 tris buffer prepared by 4 h sonication,<sup>14</sup> to which was added PS I to 1 mg mL<sup>-1</sup>. 10 μL of PS I-DMPC dispersion was evenly spread onto PG electrodes, followed by drying overnight at 4 °C in the dark. DMPC films containing heme proteins prepared in this way featured ordered lipid bilayer structures.<sup>31</sup>

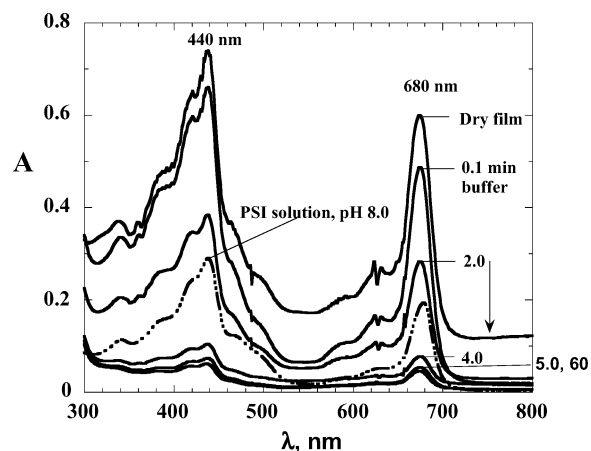


**Figure 1.** UV-vis spectra of films of dry PS I-DMPC and after wetting in 50 mM Tris buffer, pH 8.0 containing 0.1 M NaCl after 0.1, 2, 4, 5, and 60 min, shown with spectrum of PS I dissolved in pH 8.0 buffer.

**Voltammetry.** Cyclic (CV) and square wave voltammetry (SWV) on the PS I-DMPC films were done in a thermostated three electrode assembly cell at 4 °C in the dark using CHI 660A or BAS-100B electrochemical analyzers.<sup>14,32</sup> The three-electrode cell featured a saturated calomel reference electrode (SCE), a Pt wire counter electrode, and a film-coated PG electrode, and ohmic drop was compensated >95%. Potentials in this paper are reported after conversion to the NHE scale. Both CV and SWV scans were initially in positive directions from negative initial potentials, and were done in 50 mM Tris buffers, pH 8.0 containing 100 mM NaCl unless otherwise stated. Solutions were purged with purified nitrogen, and a nitrogen blanket maintained during scans. All reported results were accurately reproduced for two or more separate PS I preparations.

**Spectroscopy and Microscopy.** Absorption spectra of films on optically transparent indium tin oxide-coated (ITO) quartz slides were obtained with an HP 8453 UV-visible diode array spectrophotometer. Atomic force microscopy was done with a Nanoscope IV scanning probe microscope in tapping mode.

## Results

**Absorption Spectroscopy.** Spectral analysis (Figure 1) of dry films cast on ITO-coated quartz slides and the same films wet in pH 8 buffer solution gave characteristic strong absorption bands at 680 and 440 nm, nearly identical to native PS I dissolved in pH 8 buffer. Although it would be of interest to identify absorption characteristics of all of the cofactors in PS I in the film, this is precluded by strong background absorption due to the numerous antenna chlorophylls in PS I.<sup>33</sup> Furthermore, PS I-DMPC films on ITO quartz slides thin when soaked in buffer resulting in a decrease in absorbance, as seen previously in protein-DMPC films.<sup>34</sup> However, spectra suggest that the reaction center complex (PS I) in the PS I-DMPC films is in native state, and that the film is relatively stable on these slides after about 5 min. in buffer.

**Atomic Force Microscopy.** Films of PS I-DMPC were prepared on pyrolytic graphite (PG) disks with half of the disk

(24) Warren, P. V.; Parrett, K. G.; Golbeck, J. H.; Warden J. T. *Biochemistry* **1993**, *32*, 849–857.

(25) Scheller H. V.; Svendsen, I.; Moller, B. L. *J. Biol. Chem.* **1989**, *264*, 6929–6930.

(26) Bengis, C.; Nelson, N. J. *J. Biol. Chem.* **1975**, *264*, 2783–2788.

(27) Das, S. K.; Frank, H. A. *Biochemistry*, **2002**, *41*, 13 087–13 095.

(28) Høj, P. B.; Svendsen, I.; Scheller, H. V.; Møller, B. L. *J. Biol. Chem.* **1987**, *262*, 12 676–12 684. (b) Oh-Okada, H.; Takahashi, Y.; Wada, K.; Matsubara, H.; Ohyama, K.; Ozeki, H. *FEBS Lett.* **1987**, *218*, 52–54.

(29) Golbeck, J. *Biochim. Biophys. Acta* **1987**, *895*, 167–204.

(30) Rusling, J. F.; Zhou, L.; Munge, B.; Yang, J.; Estavillo, C.; Schenkman J. B. *Faraday Discuss.* **116**, **2000**, 77–87.

(31) Rusling, J. F. *Acc. Chem. Res.* **1998**, *31*, 363–369.

(32) Zhang, Z.; Chouchane, S.; Magliozzo, R. S.; Rusling, J. F. *Anal. Chem.* **2002**, *74*, 163–170.

(33) Brettel, K.; Leibl, W. *Biochim. Biophys. Acta* **2001**, *1507*, 100–114.

(34) Zhang, Z.; Rusling, J. F. *Biophys. Chem* **1997**, *63*, 133–146.



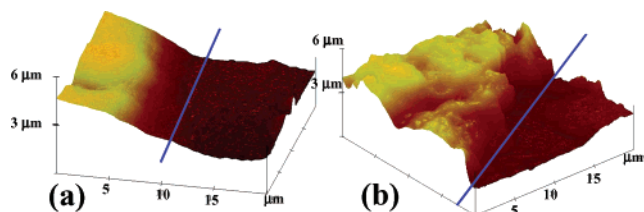


**Figure 2.** Tapping Mode Atomic Force Microscopy (AFM) images of (a) PS I/DMPC film cast on a half-masked PG disk, after stripping away the mask. Blue lines show the edge of the mask before stripping. The darker part of the image is the stripped region where no film is present, and the brighter part is where film remains. Analysis of the step suggested a film thickness of  $\sim 2.0 \pm 0.8 \mu\text{m}$ , and (b) PS I/DMPC film on a half-masked PG disk after exposure for 5 min to pH 8 buffer, then stripping away the mask, showing film reorganization to a rougher surface but no significant thinning.

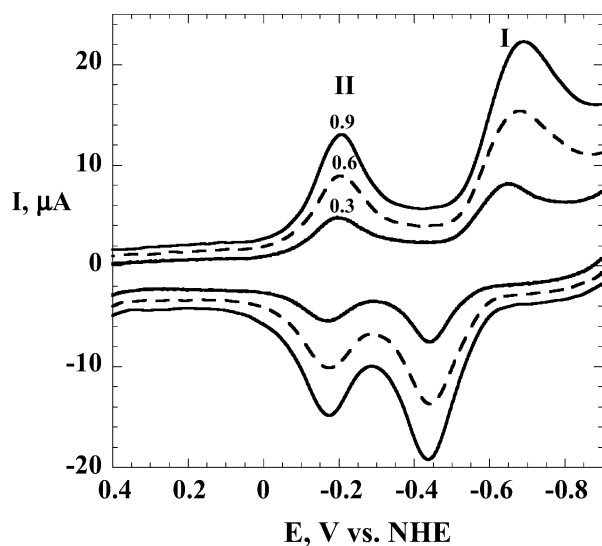


**Figure 3.** Background subtracted cyclic voltammograms (CVs) of PS I-DMPC film on PG electrode in anaerobic pH 8.0 buffer containing 100 mM NaCl at scan rates in  $\text{V s}^{-1}$  denoted on the curves.

surface masked with Teflon tape. The films were prepared as usual on this surface, and the tape was stripped off before AFM analysis. Steps connecting dark (no film) and light (film) areas of Figure 2 are indicative of the thickness of the films. Analysis of the step height in several regions suggested a film thickness  $\sim 2 \mu\text{m}$ . After the films has been exposed to buffer for 5–60 min, the film thickness did not change significantly, but the film reorganized somewhat and shows greater roughness.

**Thin Film Voltammetry.** Steady state cyclic voltammograms (CV) of films made with native PS I and DMPC (Figure 3) were stable in pH 8 buffer, and gave two well-defined chemically reversible peak pairs, I and II, in oxygen-free buffers. These peaks showed little change over 7 days storage in buffer in the dark at  $4^\circ\text{C}$ . CVs of DMPC films without PS I were featureless in this potential range.

The redox couple I had its oxidation peak at  $-0.470 \text{ V}$  (all vs NHE) and a corresponding reduction peak at  $-0.613 \text{ V}$  at  $0.10 \text{ V s}^{-1}$ . The redox couple had a formal potential ( $E^{\circ'}$ ) of  $-0.542 \text{ V}$ , estimated as the average midpoint potential between the oxidation and the reduction peak.

Redox couple II gave oxidation–reduction peaks at  $0.10 \text{ V s}^{-1}$  at  $-0.180 \text{ V}$  and  $-0.197 \text{ V}$  respectively, and a formal (midpoint) potential of  $-0.189 \text{ V}$ . CVs had nearly symmetrical peak shapes, and roughly equal reduction and oxidation peak

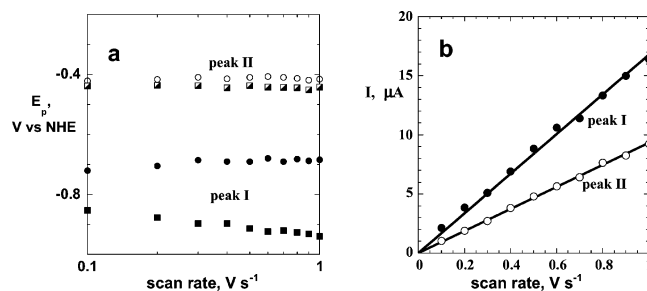


**Figure 4.** CV results for PS I-DMPC films at pH 8 for redox couples I and II: (a) Peak potentials vs log scan rate; reduction peaks are the more negative members of the peak pairs. (b) reduction peak current versus scan-rate.

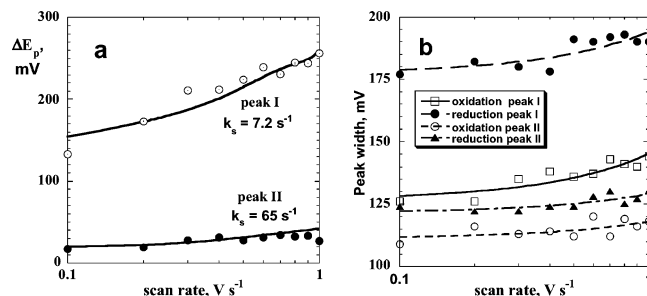


**Figure 5.** Influence of CV scan rate for PS I-DMPC films in pH 8 buffer +  $0.1 \text{ M NaCl}$  (a) on experimental ( $\odot, \bullet$ ) peak separation ( $\Delta E_p$ ) shown with theoretical lines for peak I at  $k_s = 7.2 \text{ s}^{-1}$  and for peak II at  $k_s = 65 \text{ s}^{-1}$  and (b) on peak width at half-height for peaks I and II. Calculations assumed transfer coefficient  $\alpha = 0.5$ , and used data compensated by subtracting  $\Delta E_p$  at  $0.1 \text{ V s}^{-1}$ .

currents (Figure 3). From integration of CVs of PS I-DMPC reduction peaks at low scan rates assuming one-electron reactions, average surface concentration ( $\Gamma_7$ ) was  $8.8 \pm 2.9 \times 10^{-10} \text{ mol cm}^{-2}$  for I and  $3.2 \pm 1.0 \times 10^{-10} \text{ mol cm}^{-2}$  for II.

The peak separation ( $\Delta E_p$ ) for the redox couple I was  $0.133 \text{ V}$  at  $0.1 \text{ V s}^{-1}$ , and was similar at smaller scan rates. Oxidation and reduction peak potentials of I varied in opposite directions with scan rate, with the net effect of increasing the peak separation (Figure 4a). Peak heights increased linearly with scan rate up to  $1.0 \text{ V s}^{-1}$  (Figure 4b). Peak widths at half-height were greater than the theoretical  $90 \text{ mV}$  expected for a reversible, one electron surface reaction,<sup>35,36</sup> and increased significantly with scan rate (Figure 5b). These data for redox couple I are consistent with kinetic limitations to electron transfer, and are consistent with predictions of the Butler–Volmer model for electron transfer between an electrode and redox sites in a thin film on an electrode. Above  $1.0 \text{ V s}^{-1}$  peaks became increasingly broad, showed signs of contributions from charge diffusion, had very large background currents, and thus quantitative measurements became highly subjective. Thus, we limited our analysis to scan rates  $\leq 1.0 \text{ V s}^{-1}$ .

Potentials of oxidation and reduction peaks of redox couple II were less dependent on scan rate than those of I. However, there was a small but consistent shift of reduction peaks to the negative and oxidation peaks to positive potentials leading to small increases in peak separation between  $0.1$  and  $1.0 \text{ V s}^{-1}$  (Figure 4a). Again we found a linear increase of reduction peak

(35) Laviron, E. *J. Electroanal. Chem.* **1979**, *101*, 19–28.

(36) (a) Murray, R. W. In *Electroanalytical Chemistry*; Bard, A. J., Ed.; Marcel Dekker: New York, 1984; Vol. 13, pp 191–368. (b) Murray, R. W. In *Molecular Design of Electrode Surfaces*; Murray, R. W., Ed.; John Wiley & Sons: New York, 1992; pp 1–48.

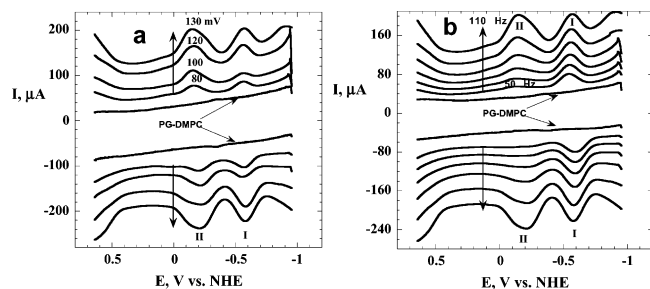


**Figure 6.** Forward (upper sets) and reverse (lower sets) SWV curves of PS I-DMPC films in anaerobic pH 8 buffer containing 100 mM NaCl: (a)  $f = 110$  Hz, Step = 4 mV, pulse height in the direction of the arrows was 80, 100, 120, and 130 mV; (b) pulse height = 130 mV, Step = 4 mV,  $f = 50, 60, 70, 80, 100,$  and  $110$  Hz in the direction of the arrows.

current with scan rate up to  $1 \text{ V s}^{-1}$  (Figure 4b). Oxidation-reduction peak separation and peak width also increased with scan rate (Figure 5).

The relatively constant peak separations found for redox couples I and II at low scan rates have been commonly observed in thin films of many redox proteins,<sup>12</sup> and may result from conformational differences between oxidized and reduced forms of the protein,<sup>37</sup> or an N-shaped potential dependence of the reaction coordinate.<sup>38</sup> Following an approach used by Hirst and Armstrong,<sup>39</sup> we compensated for the constant peak separations ( $\Delta E_p$ ) at low scan rate, and fit the corrected data to the Butler–Volmer model for electron transfer between electrode and nondiffusing redox sites.<sup>35,39</sup> Resulting fits of theory to experiment were reasonably good and provided estimates of the apparent electrochemical surface electron-transfer rate constants,  $k_s$ , which were  $65 \pm 20 \text{ s}^{-1}$  for redox couple II and  $7.2 \pm 1.3 \text{ s}^{-1}$  for redox couple I (Figure 5a).

We also used square wave voltammetry (SWV) to analyze the PS I films because it has potentially better sensitivity and resolution than CV.<sup>40</sup> SWVs (Figure 6) showed two chemically reversible redox couples I and II with midpoint potentials  $-0.550 \text{ V}$  and  $-0.200 \text{ V}$  respectively, in general agreement with CV results.

Chemical reversibility was maintained for the two redox couples at relatively large frequencies and potential pulse heights, i.e., up to 110 Hz and pulse height 130 mV. Films of DMPC alone showed no features in these potential ranges (Figure 6). Separations between forward and reverse SWV peaks for redox couples I and II were nearly zero up to 110 Hz, but at higher frequencies backgrounds became too large and peaks too broad for manageable analysis. Thus, no kinetic information could be obtained from the data at accessible frequencies. However, the lack of peak separation up to 110 Hz is consistent<sup>41</sup> with a Butler–Volmer model prediction of  $k_s \geq 10 \text{ s}^{-1}$  for both redox couples, in good agreement with CV results (cf. Figure 5a).

**PS I with Cofactors Removed.** To assign the peaks, CVs were done on PS I preparations that had been selectively

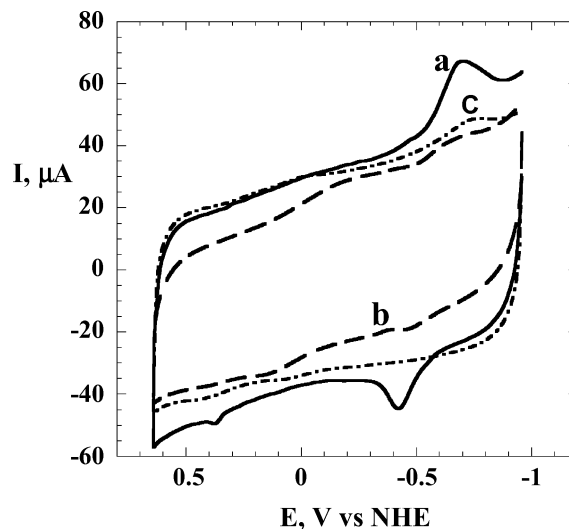


**Figure 7.** CVs at  $0.8 \text{ V s}^{-1}$  of DMPC films in anaerobic pH 8.0 buffer containing 100 mM NaCl for (a) PS I depleted of  $F_A, F_B, F_X,$  but with Pheophytin  $A_1$  cofactor present (b) PS I depleted of  $F_A, F_B, F_X,$  and  $A_1$  cofactors, and (c) DMPC film, no PS I. (Backgrounds not subtracted so as to show their shapes.)

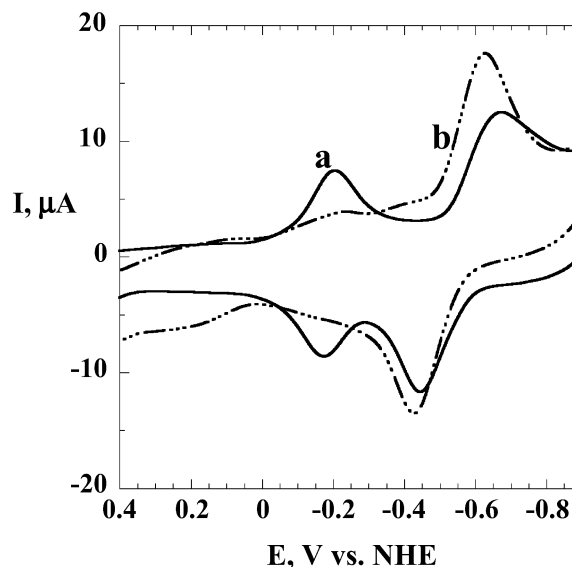


**Figure 8.** Background subtracted cyclic voltammograms at  $0.6 \text{ V s}^{-1}$  of PS I-DMPC in anaerobic pH 8.0 buffer containing 100 mM NaCl (a) native PS I (b) PS I depleted of  $F_A$  and  $F_B$  only.

depleted of specific cofactors. DMPC films with PS I depleted of  $F_A, F_B, F_X,$  but containing phytylquinone,  $A_1$  gave only one pair of oxidation–reduction peaks as opposed to two pairs of peaks for native PS I-DMPC films (Figure 7, cf. Figure 3). An oxidation peak at  $-0.467 \text{ V}$ , and a corresponding reduction peak at  $-0.579 \text{ V}$  indicated a formal potential of  $-0.523 \text{ V}$ , similar to peak I ( $E^\circ = -0.542 \text{ V}$ ) in native PS I.

In addition, Figure 7 shows CVs obtained from DMPC films containing PS I depleted of  $F_A, F_B, F_X,$  and  $A_1$ , in which no significant peaks were observed. These results suggest that the redox couple corresponding to peak I is probably due to phytylquinone  $A_1$ .

CVs of DMPC films containing PS I depleted of  $F_A$  and  $F_B$  only (Figure 8) gave no peak II, but peak I was clearly observed with oxidation peak at  $-0.461 \text{ V}$  and reduction peak at  $-0.592 \text{ V}$ . The formal potential for this redox couple is  $-0.526 \text{ V}$

- (37) El Kasmi, A.; Leopold, M. C.; Galligan, R.; Robertson, R. T.; Saavedra, S. S.; El Kacemi, K.; Bowden, E. F. *Electrochem. Commun.* **2002**, *4*, 177–181.  
 (38) Feldberg, S. W.; Rubinstein, I. *J. Electroanal. Chem.* **1988**, *240*, 1–15.  
 (39) Hirst, J.; Armstrong, F. A. *Anal. Chem.* **1998**, *70*, 5062–5071.  
 (40) Osteryoung, J.; O’Dea, J. J. In *Electroanalytical Chemistry*; Bard, A. J., Ed.; Marcel Dekker: New York, 1986; Vol. 14, pp 209–308.  
 (41) (a) Reeves, J. H.; Song, S.; Bowden, E. F. *Anal. Chem.* **1993**, *65*, 683–688. (b) O’Dea, J. J.; Osteryoung, J. *Anal. Chem.* **1993**, *65*, 3090–3097.

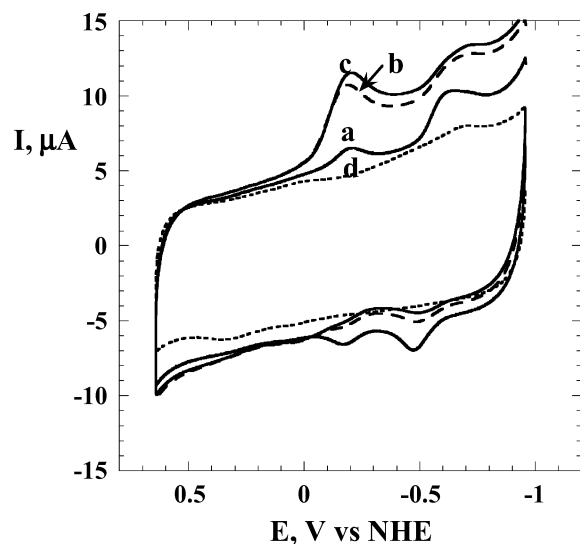


**Figure 9.** CVs at  $0.08 \text{ V s}^{-1}$  in pH 8.0 buffer of native PS I/DMPC films in anaerobic media: (a) in pH 8.0 buffer; (b) buffer +  $5.8 \mu\text{M}$  ferredoxin, (c) buffer +  $12 \mu\text{M}$  ferredoxin; and (d) PG-DMPC film control +  $12 \mu\text{M}$  ferredoxin.

compared to  $E^{\circ'} = -0.542 \text{ V}$  observed in native PS I-DMPC films. The disappearance of peak II is consistent with assignment to the  $F_A$  or  $F_B$  cofactor or both.

**Catalytic Reduction of Soluble Ferredoxin.** The terminal electron acceptor,  $F_B$  in the spinach PS I electron-transfer pathway shuttles electrons to soluble ferredoxin (Scheme 1) located on the stromal side of the PS I complex.<sup>42–45</sup> We detected this reaction by CVs of native PS I-DMPC films containing small amounts of dissolved ferredoxin in the pH 8.0 buffer. Results show an increase in current for reduction peak II at  $E^{\circ'} = -0.19 \text{ V}$ , and disappearance of the oxidation peak (Figure 9). An increase in the ferredoxin concentration increased the height of reduction peak II. This is consistent with catalytic electrochemical reduction of ferredoxin involving chemical reaction of the reduced form of redox couple II, resulting in the regeneration of its oxidized form in a catalytic cycle that increased the reduction peak height. In contrast, the reduction peak for redox couple I remains similar to before the ferredoxin addition, allowing for the larger background produced by the catalytic reduction peak II, and oxidation peak I is still visible. Although there are small changes in the CVs of I that may reflect slow reaction of ferredoxin with reduced redox couple I, any reaction would be much slower than that of reduced II. DMPC films without PS I show no peaks with or without ferredoxin in the solution.

## Discussion

Results presented above demonstrate direct electron transfer between electrodes and PS I reaction center proteins imbedded in stable biomimetic lipid films. AFM studies suggest that the films develop relatively rough surfaces during exposure to buffer. Characteristic absorbance bands observed at 680 and 440 nm in both PS I solutions and PS I-DMPC films indicate that the PS I is not significantly perturbed in the phospholipid

**Table 1.** Comparison of Midpoint Potentials in mV vs NHE for PS I Redox Cofactors in DMPC Films to Those Estimated in Solution

| sample          | P/P <sup>+</sup> | $A_1$ | $F_X/F_X^-$ | $F_A/F_A^-$ | $F_B/F_B^-$ | method                                 |
|-----------------|------------------|-------|-------------|-------------|-------------|--|
| PS I/DMPC films |                  | -542  |             | -189        | a           | CV/pH 8<br>this work                   |
| PS I/DMPC films |                  | -550  |             | -200        | a           | SWV/pH 8<br>this work                  |
| PS I/soln       | 495              | -800  | -705        | -530        | -580        | ORT <sup>b</sup> /pH 8.0 <sup>15</sup> |
| PS I/Soln       |                  |       |             | -540        | -590        | EPR at, low temp. <sup>46</sup>        |
| PS I/Soln       |                  |       |             | -440        | -465        | ORT <sup>b</sup> , RT <sup>47</sup>    |

<sup>a</sup> Discrimination between assignments to  $F_A$  or  $F_B$  could not be made.  
<sup>b</sup> ORT = optical redox titration in detergent solutions.

films. Previous infrared spectroscopic, X-ray diffraction, and calorimetric results on lipid films with and without smaller proteins such as myoglobin and cytochrome P450<sub>cam</sub> indicated that these films have structures featuring multiple stacked lipid bilayers.<sup>31</sup> We envision that the lipid films provide an environment for PS I similar to its natural membrane.

Cyclic (Figure 3) and square wave voltammetry (Figure 6) gave well-defined reversible peaks for two redox couples in the PS I-DMPC films. These peaks were assigned to phyloquinone  $A_1$  (redox couple I) and  $F_A/F_B$  iron sulfur cofactors (redox couple II) by selectively removing specific cofactors from PS I preparations, and observing the CV (Figures 7 and 8). Both of these cofactors are near the surface of the PS I complex in the membrane,<sup>2,5</sup> and we suspect that such proximity assists in their electrochemical detection in the films. By contrast, many of the other cofactors are deeply buried within the PS I complex.

Formal redox potentials of myoglobin and cyt P450<sub>cam</sub> in lipid bilayer films such as those used in the present work depended on the type of electrode material used and on specific lipid–protein interactions,<sup>31</sup> and do not correspond exactly to values from redox titrations in solution. However, in the present case, the midpoint potential ( $E_m$ ) for  $A_1$  in PS I/DMPC films by CV and SWV is about 250 mV positive of the estimated value of  $-800 \text{ mV}$  (Table 1). Similarly,  $E_m$  of  $F_A/F_B$  in our films is 240 to 340 mV more positive than values measured by optical redox titration. Thus, the redox potentials measured in the lipid films retain the quantitative relation to one another found in solution. That is, there is a 350 mV difference between the redox couples I and II in lipid films, and a 260 to 360 mV difference reported between  $A_1$  and  $F_A/F_B$  in solution (Table 1). These results suggest that  $E_m$  values obtained in the PS I/lipid films are self-consistent, and the two redox couples probably feel similar electrode double layer effects and lipid–protein interactions for both redox couples observed.

Redox couple I with a formal potential of  $-0.54 \text{ V}$  corresponds to reversible electron-transfer associated with phyloquinone redox cofactor, since PS I preparations depleted of  $F_A$ ,  $F_B$ ,  $F_X$ , but containing  $A_1$ , still gave the oxidation–reduction peaks for redox couple I (Figures 7 and 8). PS I depleted of  $F_A$ ,  $F_B$ ,  $F_X$ , and  $A_1$  gave no significant peaks over the entire potential window (Figure 7). The most likely redox reaction for I is

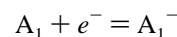


Figure 8 for PS I depleted of  $F_A$  and  $F_B$  showed only one redox couple, peak I accompanied by disappearance of peaks II at  $E_m$  0.19 V. This suggests peak assignment of redox couple II to the  $F_A$  or  $F_B$  redox cofactors, whose potentials are quite similar

(42) Vassiliev, I. R.; Sung, Y.; Yang, F.; Golbeck, J. H. *Biophys. J.* **74**, **1998**, 2029–2035.

(43) Diaz-Quintana, A.; Leibl, W.; Bottin, H.; Setif, P. *Biochemistry* **1998**, *37*, 3429–3439.

(44) He, W. Z.; Malkin, R. *Photosynth. Res.* **1994**, *41*, 381–388.

(45) Jung, Y. S.; Yu, L.; Golbeck, J. H. *Photosynth. Res.* **1995**, *46*, 249–255.

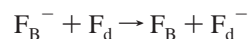
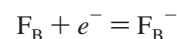
(Table 1). Possible redox reactions associated with peak II are



Voltammetric data for both of the observable PS I redox cofactors gave a good fit to the classical Butler–Volmer model of electron transfer for film-confined reactants on electrodes that assumes a simple kinetically limited electron transfer process with exponentially increasing rate constant–potential dependence.<sup>35,39</sup> Agreement of theory and experiment is illustrated by the oxidation–reduction peak separation data in Figure 5a, the analysis of which yielded apparent electrochemical rate constants of  $7.2 \text{ s}^{-1}$  for  $A_1$  and  $65 \text{ s}^{-1}$  for  $F_A/F_B$ . All of the other data in Figures 4 to 6 are also consistent with this model. That is, with increasing scan rate, oxidation and reduction peaks move in opposite directions, peak current increases linearly, and peak width increases. Although large enough frequencies in SWV could not be reached to achieve kinetic limitation without degradation of the data, the reversible voltammograms at  $\leq 110 \text{ Hz}$  are also consistent with the above model with rate constant  $\geq 10 \text{ s}^{-1}$ .

Overall, results suggest that the electrode addresses redox couples directly in PS I independent of any observable cross reactions, and that the electron-transfer processes measured at  $4 \text{ }^\circ\text{C}$  are relatively fast. Unfortunately, the lack of clearly observable kinetic limitations in SWV precluded analysis of the data with the more general Marcus theory.<sup>48</sup>

In the presence of dissolved ferredoxin (Fd), the increase in reduction peak II accompanied by disappearance of the oxidation peak (Figure 9) is characteristic of an electrochemical catalytic process<sup>12</sup> in which fast reduction of ferredoxin in solution occurs by the reduced form of iron sulfur cluster  $F_B$  and/or  $F_A$  in the PS I/DMPC film. The catalytic reaction observed by CV is suggested to be



The large current increase in response to only micromolar quantities of ferredoxin in solution attests to the high efficiency of this reaction. Previous studies of  $F_B$ -depleted PS I showed that steady-state rates of electron transfer from plastocyanin to  $\text{NADP}^+$  or to ferredoxin in spinach PS I and from cytochrome  $C_6$  to  $\text{NADP}^+$  or flavodoxin in *Synechococcus sp.* PCC 6301 PS I were inhibited by  $\sim 70\%$ , suggesting the major role played by  $F_B$ .<sup>44,45</sup> Interestingly,  $\text{NADP}^+$  reduction was completely restored upon rebuilding the  $F_B$  cluster, implying that  $F_B$  functions as the terminal electron acceptor bound to PS I. Recent studies of  $\text{P700}^+$  reduction by external electron donors<sup>42</sup> clearly showed that  $F_B$  is required for forward electron transfer to ferredoxin or flavodoxin. Most importantly, these results eliminated any ambiguity associated with a lower efficiency of electron-transfer being caused by irreversible loss of the ferredoxin and flavodoxin docking site.<sup>43,44</sup>

In summary, well-defined chemically reversible voltammetric peaks for PS I in lipid films on pyrolytic graphite electrodes were observed by voltammetry and assigned to phylloquinone  $A_1$  ( $E_m = -0.54 \text{ V}$ ) and iron sulfur clusters  $F_A/F_B$  ( $E_m = -0.19 \text{ V}$ ). On the basis of analysis with the Butler–Volmer electron-transfer model, the electrode reaction of  $F_A/F_B$  was about 10-fold faster than that of  $A_1$ . Furthermore, electron shuttle from the terminal PS I cofactor to soluble ferredoxin was observed electrochemically. The reversible voltammetry of stable PS I/lipid films described herein suggests applicability for further detailed studies of the observable cofactors in plant photosynthetic reaction centers.

**Acknowledgment.** This work was supported by the US Department of Agriculture (USDA) through Grant No. 2002-35318-12484. Its contents are solely the responsibility of the authors and do not necessarily represent the official views of USDA.

JA036671P

(46) Brettel, K. *Biochim. Biophys. Acta* **1997**, *1318*, 322–373.

(47) Jordan, R.; Nessler, U.; Schlodder, E. In *Photosynthesis: Mechanism and effects*; Garab, G., Ed.; Kluwer Academic Publishers: Dordrecht, 1998, Vol. 1, pp 663–666.

(48) Saccucci, T. M.; Rusling, J. F. *J. Phys. Chem. B* **2001**, *105*, 6142–6147.